energies

MDPI

Article

A Novel Encapsulation Method for Phase Change Materials with a AgBr Shell as a Thermal Energy Storage Material

Huanmei Yuan, Hao Bai *, Minghui Chi, Xu Zhang, Jian Zhang, Zefei Zhang and Liyun Yang

School of Metallurgical and Ecological Engineering, University of Science and Technology Beijing, No. 30 Xueyuan Road, Haidian Distinct, Beijing 100083, China; b20160123@xs.ustb.edu.cn (H.Y.); g20188228@xs.ustb.edu.cn (M.C.); zhangxu@xs.ustb.edu.cn (X.Z.); zhangjian606589@126.com (J.Z.); zhangzefei@xs.ustb.edu.cn (Z.Z.); wendy6393@163.com (L.Y.)

* Correspondence: baihao@metall.ustb.edu.cn; Tel.: +86-10-6233-2295

Received: 8 January 2019; Accepted: 19 February 2019; Published: 22 February 2019

Abstract: Micro/nanoencapsulated phase change materials, used typically as energy storage materials, are frequently applied in energy-saving and energy-efficient processes. In this work, we proposed a novel method for the micro/nanoencapsulation of phase change materials (PCMs), which has the advantage of simple operation and can be suitable for encapsulation of more than one PCM. Fatty acid PCMs, such as steric acid and palmitic acid, and non-fatty acid PCMs, like beeswax, have both been successfully micro/nanoencapsulated by a silver bromide (AgBr) shell with this method. The obtained fatty acid/AgBr micro/nanocapsules, with diameters of less than 1 μm, show good thermal storage capacities over 150 J/g with their encapsulation ratios as high as 92.4%. Similarly, the prepared beeswax/AgBr micro/nanocapsules show a high encapsulation ratio. In addition, all the micro/nanocapsules exhibit good thermal stability. Therefore, the method developed by this work is highly-efficient for the encapsulation of PCMs, which is beneficial for PCMs in various applications as energy storage materials.

Keywords: energy storage; phase change materials; AgBr shell; fatty acid; encapsulation

1. Introduction

Nowadays, the major issues to be settled urgently in the process of human sustainable development are the increasing energy crisis, high cost of fossil fuels, and environmental problems [1–4]. Phase change material (PCM), as an environmentally friendly energy storage material that can absorb/release large amounts of thermal energy during its phase transition process [5], is conducive to making energy utilization more efficient and eliminating the mismatch between energy generation and consumption [6], and therefore it is particularly important in the energy-saving process [7–10].

To date, numerous PCMs have been developed [11], and the most commonly used are some organic solid-liquid PCMs, like fatty acids and paraffin, which have superior properties such as a high thermal storage capacity, good chemical stability, little or no super-cooling, well-defined phase-change temperatures, and so on [12]. However, the direct utilization of these organic PCMs for thermal storage is limited due to the leakage problem during their solid−liquid phase transition [13].

To solve this problem, encapsulation technology has been developed by coating the PCMs core within a tiny container shell, which can prevent the PCMs from reacting with the outside environment and controlling the volume change of the PCMs during phase transition [14]. So far, several methods have been studied for the preparation of micro/nanoencapsulated PCMs, such as spray drying [15], mini-emulsion polymerization [16–18], interfacial polymerization [19], in situ polymerization [20,21],

and sol–gel method [22–25]. The shell materials for these methods contain polymer materials, such as polystyrene, poly (methyl methacrylate), melamine-formaldehyde resin, urea-formaldehyde resin, and inorganic materials such as silicon dioxide and zirconium dioxide. However, the preparation processes of these methods are complicated and the synthesis conditions are difficult to control. Take the sol–gel method as an example, during the preparation process of micro/nanocapsules, PCMs are first needed to be emulsified by the action of surfactants to form the emulsion droplets. Then sol solutions are required to be prepared with shell material (such as SiO_2) precursors (such as tetraethyl orthosilicate), catalysts, and solvents. After the sol solution has reacted for a suitable time, it is added drop-wise to the prepared emulsion to form micro/nanocapsules within a long period of time. Throughout the process, the dropping speed, type and concentration of catalyst, and ratio of substance added need to be strictly controlled, a slight error may lead to the failure [25] to form spherical core-shell structures, or may lead to the nucleation of shell materials. In addition, during the preparation of sol solutions, a large amount of solvents (mainly alcohols) are needed that will eventually be removed, which resulted from the material waste.

In this study, we proposed a novel method for the encapsulation of PCMs with a silver bromide (AgBr) shell. The formation of an AgBr shell was the result of a precipitation reaction between silver nitrate and potassium bromide, which were both employed as chemical reagents in our experiment. It is a new kind of shell material for PCMs and has shown some good performances that need further study. The preparation process can be simply divided into two steps: the first step is mainly the preparation of PCM emulsion, which is similar to other methods; the second step is adding silver nitrate solution to the emulsion to react with the potassium bromide that was initially added, and thus form silver bromide, which is then precipitated onto the emulsion surface to form a silver bromide shell. This method does not require a catalyst or any unnecessary solvents to assist the preparation process. The reaction principle is simple and the preparation conditions are easy to control. Additionally, the stable preparation process can be applied to more than one kind of PCM with maintain high encapsulation ratio. The micro/nanocapsules with good thermal storage performances obtained from this novel process can be potentially applied to thermal energy storage systems.

2. Materials and Methods

2.1. Materials

Silver nitrate ($AgNO_3$), hexadecyl trimethyl ammonium bromide (CTAB, $C_{19}H_{42}BrN$), potassium bromide (KBr), and hydroquinone were purchased from Shanghai Chemical Reagent Company, China. Stearic acid ($C_{18}H_{36}O_2$, SA), palmitic acid ($C_{16}H_{32}O_2$, PA, CP), and beeswax were bought from Beijing Chemical Reagent Company. All chemicals were used as received.

2.2. Preparation Process

In this procedure, 0.4 g of PCM was added into 50 mL of KBr aqueous solution containing 2 mM of CTAB. The mixture was then heated in a water bath at 75 °C. After the PCM became molten and floated on the surface of water, the mixture was stirred with a speed of 1500 r/min using a motor agitator at 75 °C for approximately 1 h until the oil-in-water (O/W) emulsion was formed. Afterwards, the water bath was switched off and the heating reduced. The stirring speed was reduced to 500 rpm/min, and then 10 mL of $AgNO_3$ solution was added drop-wise into the emulsion. The resultant light-yellow emulsion was stirred for another 24 h. Finally, the mixture in the beaker was washed with distilled water and centrifuged, and the powder was collected and dried at 50 °C for 24 h. Three types of samples were prepared with different PCMs (SA, PA and beeswax) by adjusting the concentrations of $AgNO_3$ solution, as shown in Table 1.

Table 1. Preparation of the samples with different phase change materials (PCMs) (Stearic acid (SA), palmitic acid (PA), and beeswax) by adjusting the concentrations of silver nitrate and potassium bromide in solutions.

PCM (g)	Samples	C_{KBr} (mM)	C_{AgNO_3} (mM)
SA	S1	18	80
	S2	54	240
PA	P1	18	80
	P2	54	240
Beewax	b1	18	80
	b2	36	160
	b3	54	240
	b4	72	400

Figure 1 shows a synthesis schematic of the micro/nanocapsules. Fatty acids and beewax are not soluble in water. When these PCMs were dispersed in the water solution containing CTAB as the surfactant, a stable O/W emulsion was produced by stirring, in which the hydrophobic segments of the emulsifiers are oriented into the oil droplets of PCMs, meanwhile, the hydrophilic segments of them are associated with the water molecules away from the oil phase. As a result, an emulsifier layer was formed to cover the surface of the oil droplets of PCMs. When $AgNO_3$ was added into the emulsion system, AgBr particles were formed by the reaction of KBr and $AgNO_3$, which were negatively charged (molar ratio of 0.8~1 for Ag+ to Br-), and then adsorbed onto the positively charged surfaces of droplets through electrostatic attraction. After enough time, a layer of AgBr shell formed on the surface of the phase change emulsion droplet.

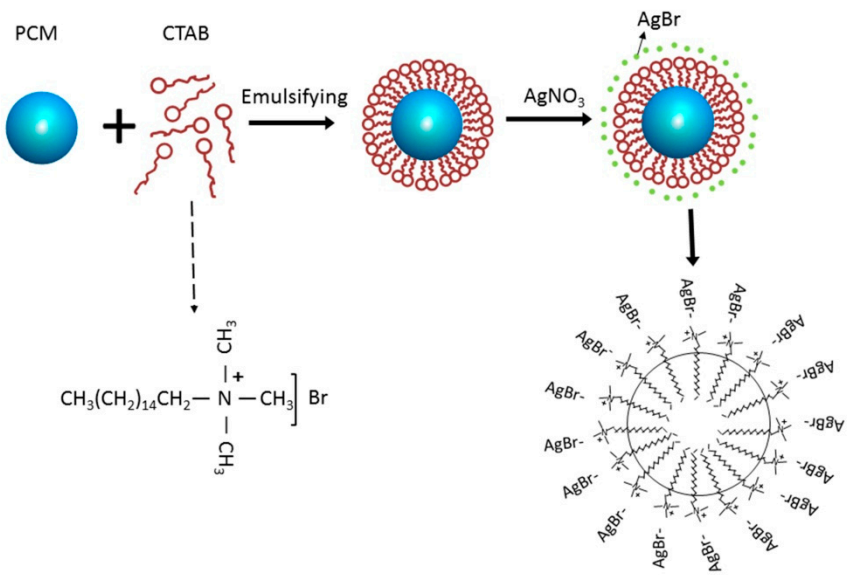

Figure 1. A synthesis schematic of the formation of fatty acid/AgBr micro/nanocapsules.

2.3. Characterization

The morphologies of the samples were observed using field-emission scanning electron microscopy (FESEM, Hitachi S-4800), and the samples were gold-coated to enhance their electrical conductivity. The core and shell structure of the samples were observed by transmission electron microscopy (TEM, FEI Tecnai G2 F20). The phase change properties and thermal stability of the samples were respectively measured by differential scanning calorimetry (DSC, Pyris Diamond) and thermogravimetric analysis (TG, METTLER 1 SF1382) at a heating rate of 10 °C/min under a purified

nitrogen atmosphere. The crystalloid phase of the samples was carried out by X-ray diffractometry (XRD, Smart Lab) at a speed of 10°/min with scanning angle 2θ ranging from 10° to 90°.

3. Results

3.1. Morphologies and Particle Sizes of the Micro/Nanocapsules

The morphology and microstructure of the prepared samples were observed by the FESEM images, as shown in Figures 2 and 3. FESEM images in Figure 2 show that the prepared samples with fatty acid are composed of irregular sphere particles with the diameters of approximately 600 nm. For SA/AgBr micro/nanocapsules, it can be observed that the particle size of S2 is relatively larger than that of S1, and so is the fact with that of P1 and P2. This indicates that with the increase of C_{KBr} and C_{AgNO3} added in the preparation process, the size of the particle increases. It is noteworthy that all these particles have coarse surfaces and present some conglutination with each other, which may be because the rapid diffusion of the AgBr particles toward the surface of the fatty acid emulsions droplets.

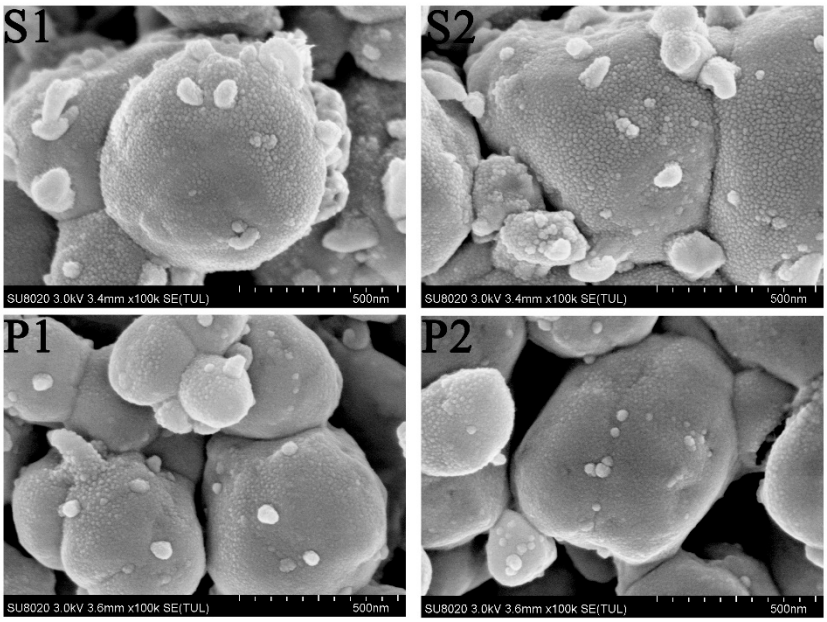

Figure 2. Micrographs of the prepared samples with fatty acid: (**S1**,**S2**) SA/AgBr microcapsules and (**P1**,**P2**) PA/AgBr microcapsules.

Figure 3 shows the FESEM images of the samples prepared with beeswax, which reveals spherical particles with diameters of about 1 μm. It is obvious that particle size increased from b1 to b4, which again indicates that the particle size increased with the increase of C_{KBr} and C_{AgNO3} added in the preparation process. It is noteworthy that these particles have smooth surfaces compared with the coarse surfaces in Figure 2, which may be the result of the large number of CTAB molecules attached on the surface of beeswax emulsion droplets [26–28], and the CTAB molecules would adsorb many silver bromide particles for nucleating and finally dense shells form. The encapsulation ratio of beeswax capsules is lower than that of palmitic acid (P1), which is probably because the dense-shell beeswax capsules formed needed more shell particles than the capsules of fatty acids did, which resulted in a slightly lower core material content for beeswax capsules. However, the surface of fatty acid capsules were loose and fragile, which can also be observed from the electron microscopy. This lead to the loss of phase change materials and reduced the coating rate, such as S1. Anyway, further study is needed for this discussion.

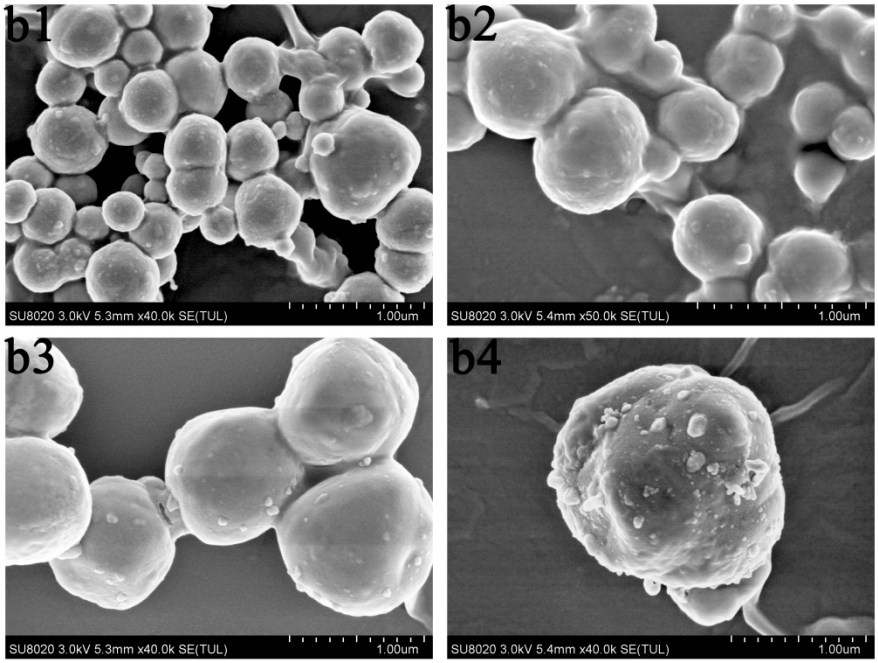

Figure 3. Micrographs of the prepared samples with beeswax with different concentrations of $AgNO_3$. (**b1**) 80 mM, (**b2**) 160 mM, (**b3**) 240 mM and (**b4**) 400 mM.

The internal microstructure of the prepared samples was confirmed by TEM, as shown in Figure 4. In Figure 4, a strong contrast between the pale ring and the dark center is evidence of the core−shell structure, which indicates the successful fabrication of microcapsules.

3.2. Crystalloid Phase of Microencapsulated PCMs with AgBr Shell

X-ray diffraction was used to determine the crystalloid phase of materials and the XRD patterns of pure PCMs (SA, PA, beeswax), the prepared micro/nanocapsules, and AgBr (JCPDS cards, No.79-0149), as shown in Figures 5 and 6. In the XRD pattern of SA in Figure 5, the peaks appear at 6.5°, 11.0°, 15.4°, 20.3°, 21.4°, 24.0°, 30°, 39.8° and 45.2° indicating regular crystallization. In particular, the two sharp diffraction peaks at 21.4° and 24.0° are characteristic peaks of SA. The XRD patterns at 10–25° of S1 and S2 are attributed to the crystal planes of SA, while the patterns at approximately 26–85° are mainly assigned to the characteristic peaks of AgBr (JCPDS cards, No.79-0149). Additionally, in the patterns of S1 and S2, new peaks at 38.1° and 77.4° appeared, which may have resulted from the formation of silver particles (PDF#87-0597) caused by the decomposition of silver bromide. Generally, results indicated that S1 and S2 are mainly composed of SA and AgBr.

Similarly, by analyzing the XRD patterns of P1, P2, and PA in Figure 5, and the XRD patterns of b1–b4 and beeswax in Figure 6, we can concluded that the samples are mainly composed of the AgBr and the corresponding PCMs. On the basis of the FESEM and TEM observations, it can be confirmed that the SA/AgBr micro/nanocapsules were obtained using the present method.

3.3. Thermal Properties of the LA/SiO_2 Nanocapsules

Phase change properties are of vital importance for the micro/nanocapsules. DSC was used to test the phase change properties of the as-prepared samples. Figures 7 and 8 present the DSC curves of SA, PA, beeswax and the prepared samples for the melting and solidifying process. Tables 2 and 3 contain the detailed data of the DSC results.

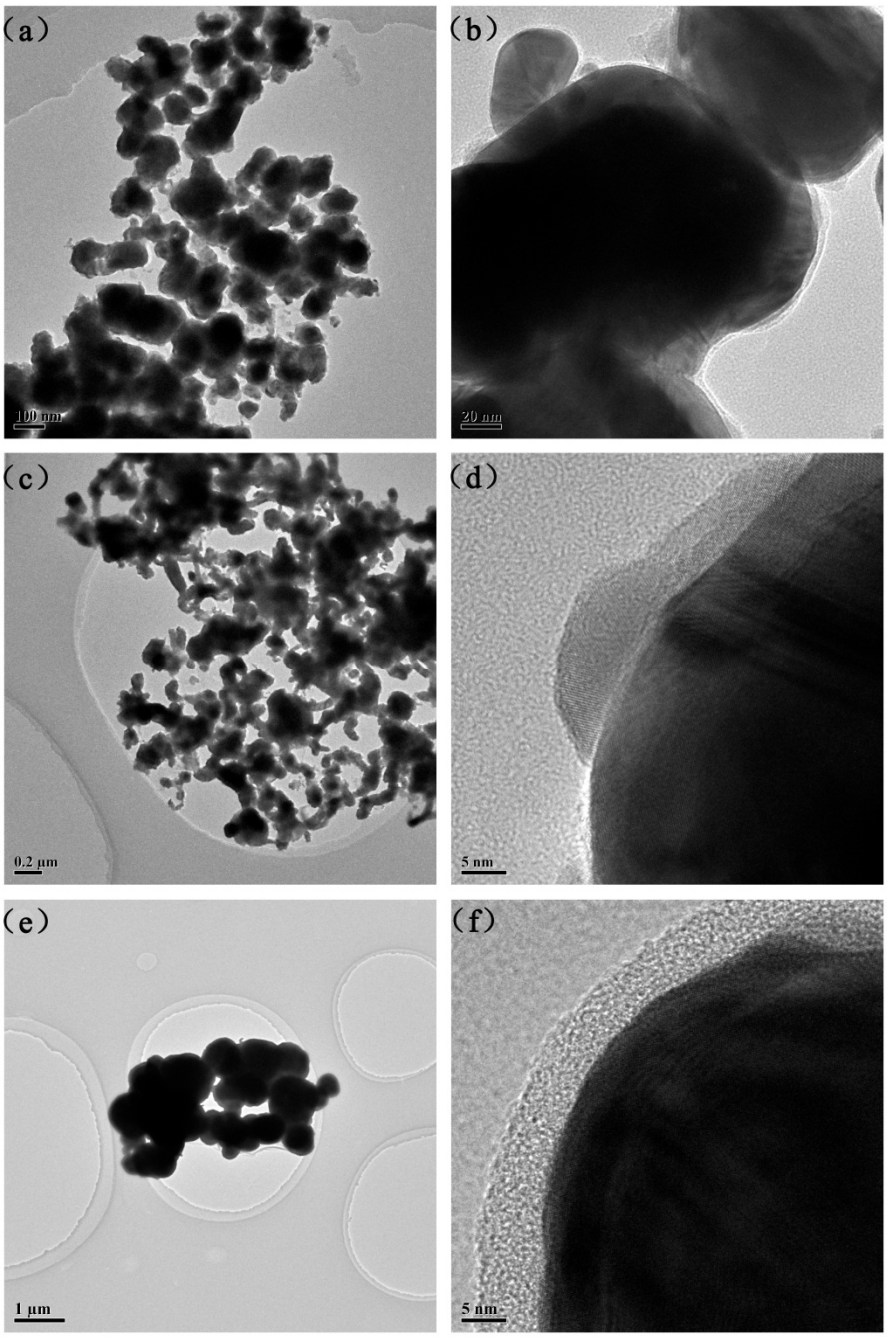

Figure 4. TEM images of the as-prepared samples: (**a**,**b**) the SA/AgBr micro/nanocapsules; (**c**,**d**) the PA/AgBr micro/nanocapsules, and (**e**,**f**) the beeswax/AgBr micro/nanocapsules.

Table 2. DSC data for the prepared fatty acid/AgBr micro/nanocapsules.

Samples	Melting		Solidifying		Encapsulation Ratio R (%)	Encapsulation Efficiency E (%)
	T_m (°C)	ΔH_m (J/g)	T_c (°C)	ΔH_c (J/g)		
Pure SA	67.0	238.7	62.5	244.1	100	100
S1	66.8	159.0	55.7	177.3	66.6	69.6
S2	67.5	29.6	58.7	26.3	28.2	11.6
Pure PA	60.4	172.1	50.1	174.4	3.7	100
P1	62.9	159.0	48.4	155.6	92.4	65.2
P2	61.4	58.7	52.1	40.7	34.1	20.6

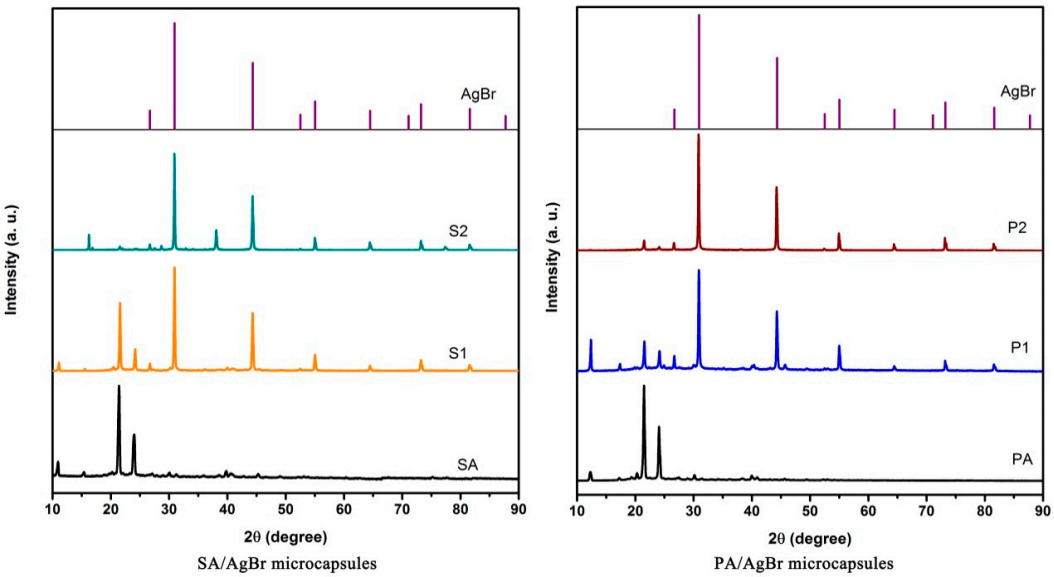

Figure 5. X-ray diffraction of SA, PA, AgBr, and prepared nanocapsules.

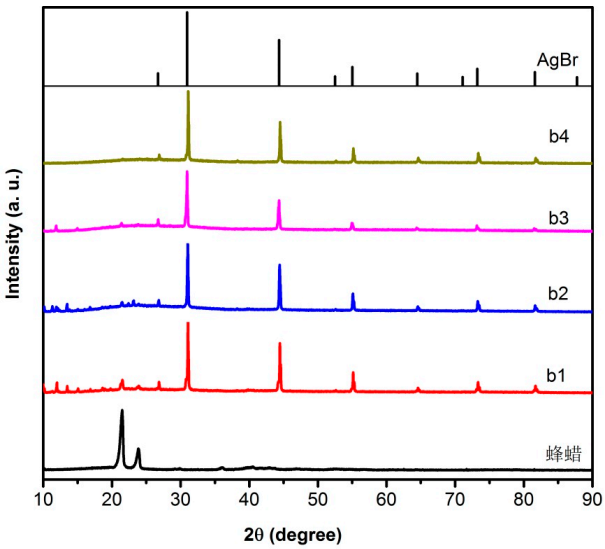

Figure 6. X-ray diffraction of the beeswax/AgBr microcapsules.

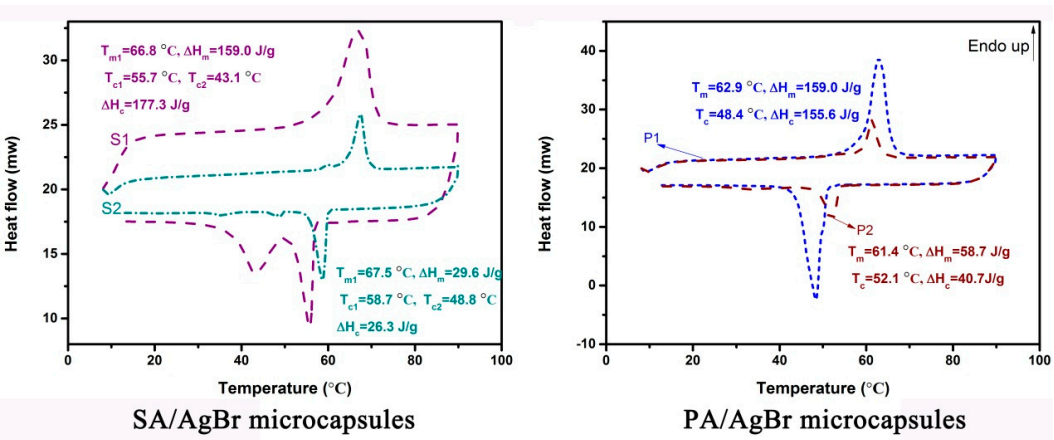

Figure 7. The melting and solidifying DSC curves for the S1, S2, P1, and P2.

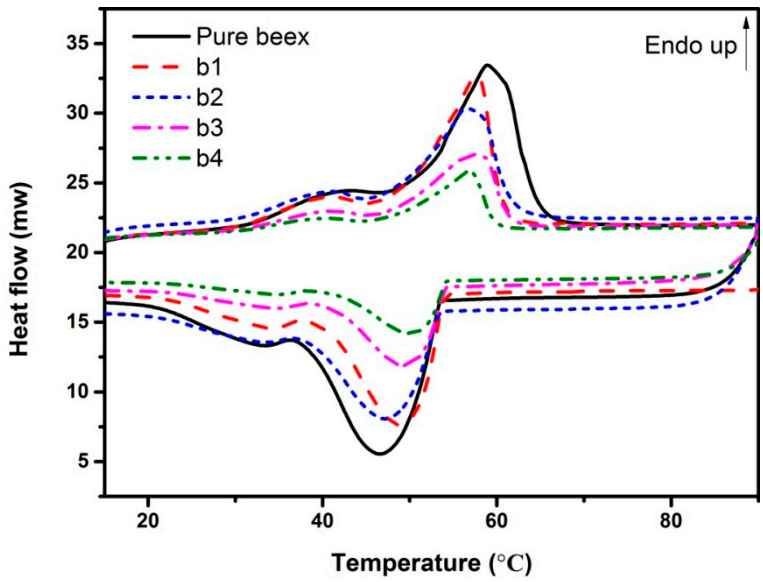

Figure 8. The melting and solidifying DSC curves for the beeswax/AgBr microcapsules.

Table 3. DSC data for the prepared beeswax/AgBr micro/nanocapsules.

Samples	Melting		Solidifying		Encapsulation Ratio R (%)	Encapsulation Efficiency E (%)
	T_m (°C)	ΔH_m (J/g)	T_c (°C)	ΔH_c (J/g)		
beeswax	58.9	119.3	46.5	128.6	100.0	100.0
b1	57.9	99	49	107.3	83.0	83.2
b2	56.3	73	47.2	77.2	61.2	60.6
b3	56.9	65.2	50.4	69.9	54.7	54.5
b4	57.1	45.3	49.4	47.2	38.0	37.3

As shown in Tables 2 and 3, the melting and solidifying temperatures of the prepared samples are close to those of the pure PCMs. The latent heats of the micro/nanocapsules during the melting and solidifying process changes with the concentrations of silver nitrate and potassium bromide in solutions. Encapsulation ratio (R) and encapsulation efficiency (E) were calculated according to the following Equations [12]:

$$R = \frac{\Delta H_{m,EPCMs}}{\Delta H_{m,PCMs}} \times 100\% \quad (1)$$

$$E = \frac{\Delta H_{m,EPCMs} + \Delta H_{c,EPCMs}}{\Delta H_{m,PCMs} + \Delta H_{c,PCMs}} \times 100\% \quad (2)$$

where $\Delta H_{m,PCMs}$ and $\Delta H_{c,PCMs}$ are the latent heats of the PCMs during the melting and solidifying process, respectively. $\Delta H_{m,EPCMs}$ and $\Delta H_{c,EPCMs}$ are the latent heats of the micro/nanocapsules during the melting and solidifying process. R indicates the effective encapsulation of core materials within the micro/nanocapsules, and E reflects the effective performance of the micro/nanocapsules for thermal storage. In Table 2, it shows that the maximum encapsulation ratio of SA/AgBr micro/nanocapsules and PA/AgBr micro/nanocapsules is 66.2% and 92.4%, respectively. By increasing the concentrations of silver nitrate and potassium bromide in solutions (S1-S2, P1-P2), the encapsulation ratios of SA/AgBr micro/nanocapsules and PA/AgBr micro/nanocapsules reduced to 28.2% and 34.1%, respectively, which indicates that high concentrations of silver nitrate and potassium bromide during the preparation process may lead to the decrease of the encapsulation ratios of micro/nanocapsules.

This can be confirmed by the change of encapsulation ratios of beeswax/AgBr micro/nanocapsules, as shown in Table 3. The highest encapsulation ratio of beeswax/AgBr micro/nanocapsules was 83.0%, which were prepared with the minimum concentrations of

silver nitrate and potassium bromide in the four samples. The encapsulation ratio decreased gradually (b1–b4) with increasing concentrations of silver nitrate and potassium bromide. Results indicate that a high concentration of silver nitrate and potassium bromide is not beneficial to the encapsulation ratio of micro/nanocapsules, which may be related to the large proportion of AgBr material in the micro/nanocapsules. The encapsulation method for this work obtained phase change micro/nanocapsules with high encapsulation ratio (i.e., PA/AgBr and beeswax/AgBr micro/nanocapsules could be as high as 92.4% and 83.0%, respectively, that is, the reductions of latent heat is only 7.6% for PA and 17% for beeswax, after they are encapsulated), which show advantages compared with other methods, as shown in Table 4. As for SA/AgBr micro/nanocapsules with an encapsulation ratio of 66.6%, which is in the middle level compared with that of other methods, and this may be related to the composition of the substance and needs to be further optimized. All in all, the SA/AgBr micro/nanocapsules, PA/AgBr micro/nanocapsules and beeswax/AgBr micro/nanocapsules prepared in this work have a high thermal storage capacity.

Table 4. Comparison of the encapsulation ratio of the micro/nanocapsules prepared in this work with that of other methods.

Materials	Preparation Methods	R (%)	Reference
Paraffin/ PMMA	Mini-emulsion polymerization	60.7	[29]
Paraffin/polyurea	Interfacial polymerization	66.6	[30]
EA-SA/PMMA	Emulsion polymerization	65.2	[31]
n-dotriacontane/PS	Mini-emulsion polymerization	61.2	[16]
SA/ titania	Sol-gel	64.8	[24]
PA/SiO_2	Sol-gel	90.0	[23]
n-octadecane / PSDB	Interfacial polymerization on	66.5	[19]
LA/MF	In situ polymerization	46.2	[20]
Paraffin/CMC-MF	In situ polymerization	63.1	[21]
Beeswax/AgBr	New method	83.0	This work
PA/AgBr	New method	92.4	This work
SA/AgBr	New method	66.6	This work

3.4. Thermal Stability of the Microcapsules

The thermal stability is an important feature for the micro/nanocapsules used for thermal regulation or thermal energy storage. TG curves of the as-prepared samples S1 and S2, P1 and P2, b1–b4, and the pure PCMs are shown in Figures 9 and 10.

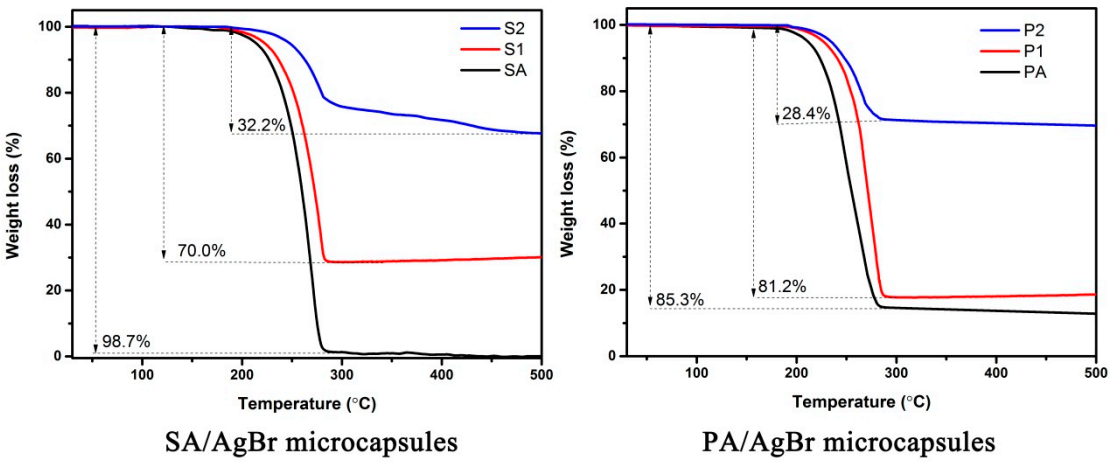

Figure 9. Define. curves for the SA/AgBr microcapsules and PA/AgBr microcapsules.

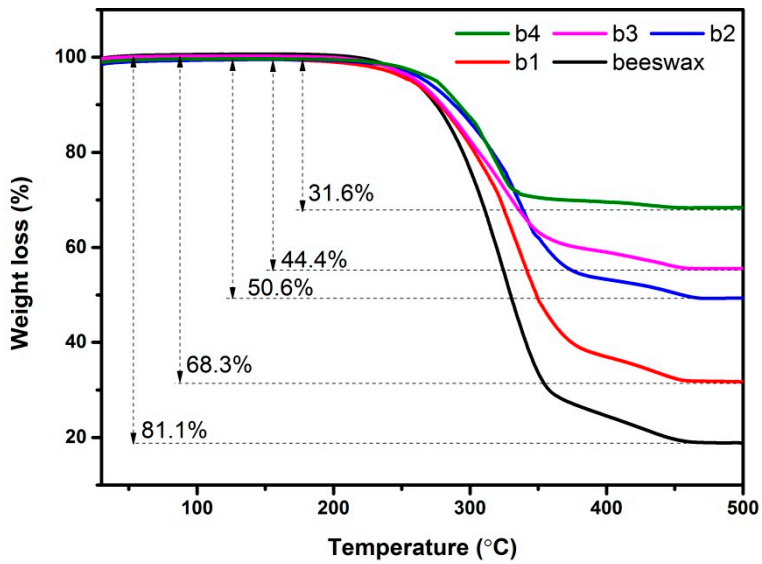

Figure 10. TG curves for the beeswax and beeswax/AgBr microcapsules.

For the SA and the SA/AgBr micro/nanocapsules in Figure 9, it is obvious that the thermal stability is the worst for SA, which exhibits a simple evaporation process above 185 °C, and the weight loss is 98.7%. As for the SA/AgBr micro/nanocapsules, we can observe similar decomposition processes above 195 °C, which is attributed to the decomposition of the micro/nanoencapsuled SA. The weight loss of S1 and S2 is 70% and 32.2%, respectively, which is quite possibly due to the decreased content of SA. Similarly, for the PA and PA/AgBr micro/nanocapsules in Figure 9, the pure PA starts to be removed at about 181 °C, and the final weight loss percentage is 85.3% at 286 °C. In the TG curves of P1 and P2, the weight loss percentage during the temperature range of 189–287 °C and 192–289 °C is about 81.2% and 28.4%, respectively, which is attributed to the removal of PA in the PA/AgBr micro/nanocapsules.

As for the beeswax and beeswax/AgBr micro/nanocapsules in Figure 9, we can observe a two-stage decomposition process for the beeswax at around 210–458 °C, which may due to the fact that beeswax is not a single substance but a mixture (mainly containing esters, fatty acids and sugars), of which the degradation temperature is different for different components. It is obvious that the beeswax/AgBr micro/nanocapsules (b1–b4) showed a similar decomposition process (about 220–470 °C) with that of the pure beeswax, and their weight loss is mainly related to the content of beeswax in the micro/nanocapsules.

Additionally, all the prepared micro/nanocapsules (S1 and S2, P1 and P2, and b1–b4) exhibited an improvement in the onset temperature for the weight loss and the temperature for the maximum weight loss comparing with that of the pure PCMs. This can be explained by the fact that the AgBr shell can prevent the encapsulated PCMs from thermal degradation effectively. Moreover, the AgBr shell remained as residual char at the end of TG measurements, and the char yield increased gradually with increasing the concentration of silver nitrate and potassium bromide during the preparation of the micro/nanocapsules, as shown in Figures 9 and 10. Furthermore, the weight loss of these samples in their usage temperature range (i.e., 30–80 °C) is small, it can be inferred that these samples could also have good durability after repeated heating/cooling thermal cycles [32]. It was shown that the AgBr shells may have improved the thermal stability of PCMs in the micro/nanocapsules.

4. Discussion

A novel method has been proposed for AgBr-coated phase change materials. Fatty acid PCMs such as SA and PA have been successfully encapsulated by AgBr shell with this method. The obtained fatty acid/AgBr micro/nanocapsules with diameters of less than 1 um achieved high thermal storage

capacity over 150 J/g (S1 and P1), and their encapsulation ratio can as high as 92.4% (P1) by adjusting the synthetic conditions. In addition, this method can also be used to coat non-fatty acid phase change materials such as beeswax, and the prepared beeswax/AgBr micro/nanocapsules can also show a high encapsulation ratio (83% for b1). Therefore, the method developed by this work is suitable for more than one kind of PCM, and the preparation process is highly-efficient for the encapsulation of PCMs, which exhibits a great potential for the energy-efficient utilizations of the micro/nanocapsules.

Author Contributions: H.B. and H.Y. proposed the concrete ideas of the work; M.C. and H.Y. conducted the experiments; X.Z., J.Z. and Z.Z. devoted to the data analysis; H.B., L.Y. and H.Y. wrote the paper.

Funding: This research was financially supported by National Key R&D Program of China with the Nos. 2018YFF0216000.

Acknowledgments: The authors would like to thank the Scientific Compass and Chinese Medical Examination for their TEM and FESEM tests.

Conflicts of Interest: The authors declare no conflict of interest.

References

1. Lian, Q.; Yan, L.; Sayyed, A.A.S.; Cheng, J.; Zhang, J. Facile Strategy in Designing Epoxy/Paraffin Multiple Phase Change Materials for Thermal Energy Storage Applications. *ACS Sustain. Chem. Eng.* **2018**, *6*, 3375–3384. [CrossRef]
2. Liu, H.; Wang, X.; Wu, D. Fabrication of Graphene/TiO2/Paraffin Composite Phase Change Materials for Enhancement of Solar Energy Efficiency in Photocatalysis and Latent Heat Storage. *ACS Sustain. Chem. Eng.* **2017**, *5*, 4906–4915. [CrossRef]
3. Zhou, Y.; Liu, X.; Sheng, D.; Lin, C.; Ji, F.; Dong, L.; Xu, S.; Wu, H.; Yang, Y. Polyurethane-based solid-solid phase change materials with in situ reduced graphene oxide for light-thermal energy conversion and storage. *Chem. Eng. J.* **2018**, *338*, 117–125. [CrossRef]
4. Zhang, H.; Sun, Q.; Yuan, Y.; Zhang, Z.; Cao, X. A novel form-stable phase change composite with excellent thermal and electrical conductivities. *Chem. Eng. J.* **2018**, *336*, 342–351. [CrossRef]
5. Yuan, H.; Bai, H.; Zhang, X.; Zhang, J.; Zhang, Z.; Yang, L. Synthesis and characterization of stearic acid/silicon dioxide nanoencapsules for solar energy storage. *Sol. Energy* **2018**, *173*, 42–52. [CrossRef]
6. Jiang, Z.; Yang, W.; He, F.; Xie, C.; Fan, J.; Wu, J.; Zhang, K. Modified Phase Change Microcapsules with Calcium Carbonate and Graphene Oxide Shells for Enhanced Energy Storage and Leakage Prevention. *ACS Sustain. Chem. Eng.* **2018**, *6*, 5182–5191. [CrossRef]
7. Zhang, T.; Chen, M.; Zhang, Y.; Wang, Y. Microencapsulation of stearic acid with polymethylmethacrylate using iron (III) chloride as photo-initiator for thermal energy storage. *Chem. Eng. J.* **2017**, *25*, 1524–1532. [CrossRef]
8. Siyabi, I.A.; Khanna, S.; Mallick, T.; Sundaram, S. Multiple Phase Change Material (PCM) Configuration for PCM-Based Heat Sinks—An Experimental Study. *Energies* **2018**, *11*, 1629. [CrossRef]
9. Li, S.; Yu, C.; Sun, Z. Numerical Simulation and Optimization of the Melting Process of Phase Change Material inside Horizontal Annulus. *Energies* **2017**, *10*, 1249.
10. Akeiber, H.J.; Hosseini, S.E.; Wahid, M.A.; Mohammad, A.T. Phase Change Materials-Assisted Heat Flux Reduction: Experiment and Numerical Analysis. *Energies* **2016**, *9*, 30. [CrossRef]
11. Pielichowska, K.; Pielichowski, K. Phase change materials for thermal energy storage. *Prog. Mater. Sci.* **2014**, *65*, 67–123. [CrossRef]
12. Fang, Y.; Zou, T.; Liang, X.; Wang, S.; Liu, X.; Gao, X.; Zhang, Z. Self-assembly Synthesis and Properties of Microencapsulated n-Tetradecane Phase Change Materials with a Calcium Carbonate Shell for Cold Energy Storage. *ACS Sustain. Chem. Eng.* **2017**, *5*, 3074–3080. [CrossRef]
13. Jamekhorshid, A.; Sadrameli, S.M.; Farid, M. A review of microencapsulation methods of phase change materials (PCMs) as a thermal energy storage (TES) medium. *Renew. Sustain. Energy Rev.* **2014**, *31*, 531–542. [CrossRef]
14. Farid, M.M.; Khudhair, A.M.; Razack, S.; Al-Hallaj, S. A review on phase change energy storage: Materials and applications. *Energy* **2004**, *45*, 1597–1615. [CrossRef]

15. Teixeira, M.I.; Andrade, L.R.; Farina, M.; Rocha-Leao, M.M. Characterization of short chain fatty acid microcapsules produced by spray drying. *Mater. Sci. Eng. C* **2004**, *24*, 653–658. [CrossRef]
16. Fang, Y.; Liu, X.; Liang, X.; Liu, H.; Gao, X.; Zhang, Z. Ultrasonic synthesis and characterization of polystyrene/n-dotriacontane composite nanoencapsulated phase change material for thermal energy storage. *Appl. Energy* **2014**, *132*, 551–556. [CrossRef]
17. Liang, S.; Li, Q.; Zhu, Y.; Chen, K.; Tian, C.; Wang, J.; Bai, R. Nanoencapsulation of n-octadecane phase change material with silica shell through interfacial hydrolysis and polycondensation in miniemulsion. *Energy* **2015**, *93*, 1684–1692. [CrossRef]
18. Chen, Z.H.; Yu, F.; Zeng, X.R.; Zhang, Z.G. Preparation, characterization and thermal properties of nanocapsules containing phase change material n-dodecanol by miniemulsion polymerization with polymerizable emulsifier. *Appl Energy* **2012**, *91*, 7–12. [CrossRef]
19. Li, W.; Song, G.L.; Tang, G.Y.; Chu, X.D.; Ma, S.D.; Liu, C.F. Morphology, structure and thermal stability of microencapsulated phase change material with copolymer shell. *Energy* **2011**, *36*, 785–791. [CrossRef]
20. Bao, Y.; Pan, W.; Wang, T.; Wang, Z.; Wei, F.; Xiao, F. Microencapsulation of fatty acid as phase change material for latent heat storage. *J. Energy Eng.* **2011**, *137*, 214–219. [CrossRef]
21. Hu, X.; Huang, Z.; Zhang, Y. Preparation of CMC-modified melamine resin spherical nano-phase change energy storage materials. *Carbohyd. Polym.* **2014**, *101*, 83–88. [CrossRef]
22. Fang, G.Y.; Chen, Z.; Li, H. Synthesis and properties of microencapsulated paraffin composites with SiO2 shell as thermal energy storage materials. *Chem. Eng. J.* **2010**, *163*, 154–159. [CrossRef]
23. Latibari, S.T.; Mehrali, M.; Mehrali, M.; Mahlia, T.M.I.; Metselaar, H.S.C. Synthesis, characterization and thermal properties of nanoencapsulated phase change materials via sol-gel method. *Energy* **2013**, *61*, 664–672. [CrossRef]
24. Latibari, S.T.; Mehrali, M.; Mehrali, M.; Afifi, A.B.M.; Mahlia, T.M.I.; Akhiani, A.R.; Metselaar, H.S.C. Facile synthesis and thermal performances of stearic acid/titania core/shell nanocapsules by sol–gel method. *Energy* **2015**, *85*, 635–644. [CrossRef]
25. Zhu, Y.; Liang, S.; Wang, H.; Zhang, K.; Jia, X.; Tian, C.; Zhou, Y.; Wang, J. Morphological control and thermal properties of nanoencapsulated n-octadecane phase change material with organosilica shell materials. *Energy Convers. Manag.* **2016**, *119*, 151–162. [CrossRef]
26. Ahmad, K.; Ho, C.C.; Fong, W.K.; Toji, D. Properties of palm oil-in-water emulsions stabilized by nonionic emulsifiers. *J. Colloid Interf. Sci.* **1996**, *181*, 595–604. [CrossRef]
27. Shinoda, K.; Saito, H. The stability of O/W type emulsions as functions of temperature and the HLB of emulsifiers: The emulsification by PIT-method. *J. Colloid Interf. Sci.* **1969**, *30*, 258–263. [CrossRef]
28. Kamel, B.S. Emulsifiers. In *Food Additive User's Handbook*; Springer: Boston, MA, USA, 1991; pp. 169–201.
29. Cortazar, M.G.; Rodriguez, R. Thermal Storage Nanocapsules by Miniemulsion Polymerization. *J. Appl. Polym. Sci.* **2013**, *127*, 5059–5064. [CrossRef]
30. Park, S.; Lee, Y.; Kim, Y.S.; Lee, H.M.; Kim, J.H.; Cheong, I.W.; Koh, W.G. Magnetic nanoparticle-embedded PCM nanocapsules based on paraffin core and polyurea shell. *Colloid. Surf. A* **2014**, *450*, 46–51. [CrossRef]
31. Wang, Y.; Zhang, Y.; Xia, T.D.; Zhao, W.J.; Yang, W.H. Effects of fabricated technology on particle size distribution and thermal properties of stearic–eicosanoic acid/polymethylmethacrylate nanocapsules. *Sol. Energy Mater. Sol. Cells* **2014**, *120*, 481–490. [CrossRef]
32. Yuan, H.; Bai, H.; Lu, X.; Zhang, X.; Zhang, J.; Zhang, Z.; Yang, L. Size controlled lauric acid/silicon dioxide nanocapsules for thermal energy storage. *Solar Energy Mater. Solar Cells* **2019**, *191*, 243–257. [CrossRef]